Aleksandar Sedmak[1*], Ivana Petrović[1], Miloš Milošević[2], Calin Dascau[3], Aleksa Milovanović[2], Radun Vulović[4]

DIGITAL TWIN-BASED NUMERICAL SIMULATION OF STRESS DISTRIBUTION IN THE MANDIBLE WITH DENTAL IMPLANTS

NUMERIČKA SIMULACIJA RASPODELE NAPONA U VILICI SA ZUBNIM IMPLANTIMA ZASNOVANA NA DIGITALNOM BLIZANCU

Originalni naučni rad / Original scientific paper
Rad primljen / Paper received: 12.05.2025
https://doi.org/10.69644/ivk-2025-02-0161

Adresa autora / Author's address:
[1)] University of Belgrade, Faculty of Mechanical Engineering, Belgrade, Serbia, A. Sedmak https://orcid.org/0000-0002-5438-1895 , [*]email: aleksandarsedmak@gmail.com
[2)] Innovation Centre of the Faculty of Mech. Eng., Belgrade, Serbia, M. Milošević https://orcid.org/0000-0002-2418-1032; A. Milovanović https://orcid.org/0000-0003-4668-8800
[3)] 'Victor Babeș' University of Medicine and Pharmacy, Dept. of Internal Medicine, Timișoara, Romania
[4)] Institute for Information Technologies, Kragujevac, Serbia, R. Vulović https://orcid.org/0000-0002-5545-9965

Keywords
- digital twin
- finite element method
- stress distribution
- dental implants

Abstract

A segment of the mandible with dental implants and natural teeth is modelled in SolidWorks® to create two digital twins: one with coupled implants and the other with separated implants. These digital twins are subsequently used to develop finite element models for calculating stresses and determine the stress distribution under various loading conditions and material configurations. The modelling process is presented here in full detail, while stress analysis results are presented in detail just for the case involving separated implants, with a porcelain veneer, and the loading applied equally at two points. All the other considered eight cases are briefly presented and discussed.

Ključne reči
- digitalni blizanac
- metoda konačnih elemenata
- raspodela napona
- zubni implanti

Izvod

Segment donje vilice sa zubnim implantima i prirodnim zubima modelovan je u programu SolidWorks® kako bi se kreirala dva digitalna blizanca: jedan sa spojenim implantima i drugi sa odvojenim implantima. Ovi digitalni blizanci su zatim korišćeni za razvoj modela konačnih elemenata radi izračunavanja napona i određivanja raspodele napona pod različitim uslovima opterećenja i izbora materijala. Proces modelovanja je detaljno opisan, dok su rezultati analize napona detaljno prikazani samo za slučaj sa odvojenim implantima, sa porcelanskim fasetama, i opterećenjem ravnomerno primenjenim u dve tačke. Svi ostali razmatranih slučajevi (osam) su ukratko opisani.

INTRODUCTION

Development of oral implants has significantly advanced the rehabilitation of partially or fully edentulous patients. However, evaluating the implant behaviour *in vivo* remains a major challenge due to practical and ethical limitations. As a result, various *in vitro* experimental techniques or numerical simulations are used instead. Among experimental techniques, Digital Image Correlation (DIC) is the most widely used, while Finite Element Method (FEM) is the standard approach for numerical analysis, as shown in /1-13/.

The primary objective of numerical simulation is to determine the stress distribution within the implant and surrounding mandible, thereby improving reliability and minimising the risk of premature failure. To achieve this, two key steps are required: first, creating a geometrically identical CAD model, followed by mathematical modelling typically using FEM. The first step, i.e., creating a high-fidelity virtual representation, is nowadays often referred to as digital twinning. In this paper, two digital twins of a mandibular segment with either coupled or separated dental implants are developed in SolidWorks®, with natural teeth included in both configurations. The FEM is then employed to analyse stress the distribution across all investigated cases.

MODELLING - DIGITAL TWIN

An implant design chosen for this study is 'Titamax GT cortical' (Straumann, Basel, Switzerland), with a 3.75 mm diameter and a length of 11.0 mm. The top of the implant is grooved and has a dome shape. A particular implant belongs to the group of threaded implants with a cylindrical shape. The threads on the implant are in the form of Latin letter 'V'. The neck surface of the implant is polished, and it has a larger diameter than the body of the implant, 4.8 mm. In this study, the threads are omitted for easier result analysis, and the implant is designed as a solid cylindrical structure with dimensions Ø3.75 × 11 mm. In addition, the presence of an abutment is disregarded for easier numerical analysis.

In the scope of this study, two simplified models are developed based on models presented in /2-4/, with modifications of veneer materials and the number of load application points. Figure 1a shows their physical model with coupled crowns, while Fig. 1b depicts the model with separated crowns. The CAD models are created in SolidWorks (Dassault Systèmes, Vélizy-Villacoublay, France). Both models consist of a block into which the first premolar, second molar, and two implants with crowns are inserted at the positions of the second premolar and the first molar. The only difference between the models is in the crowns: in the first model, they are coupled, while in the other model, they are separated. The construction of the assembly model with separated crowns can be presented in 6 stages: 1. first premolar, 2. second molar, 3. implants, 4. crown for the second premolar, 5. crown for the first molar, and 6. final assembly.

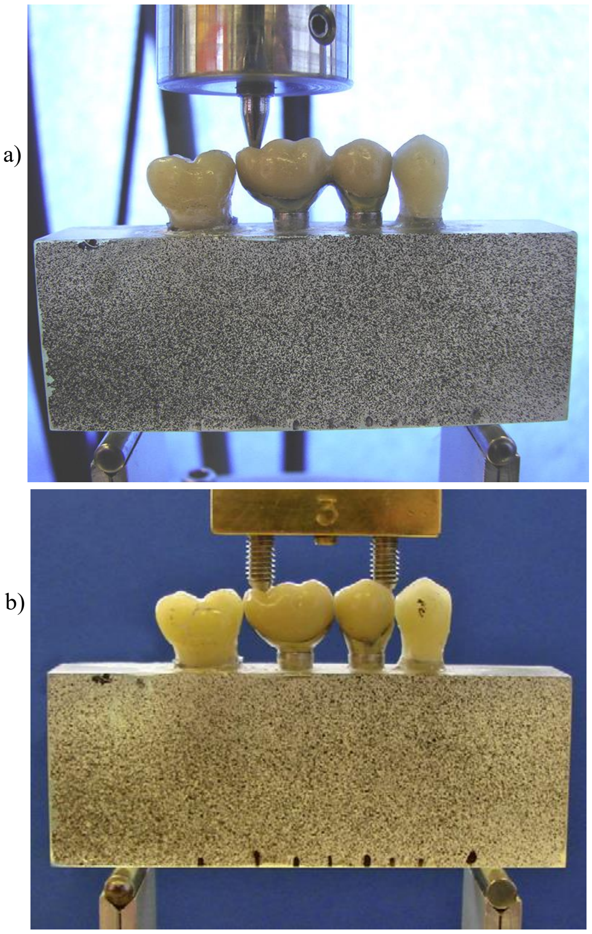

Figure 1. Physical model: a) coupled; b) separated abutments, /1/.

The tooth model was constructed in two steps. The first step involved the creation of dentin, followed by the construction of enamel in the second step. Due to irregular geometry, it was constructed using eight parallel planes aligned with the *Top plane* in SolidWorks® software. An initial 2D sketch of the dentin and enamel created in the *Front plane* in SolidWorks, with eight marked parallel construction planes, is shown in Fig. 2a. For clarity, the seven auxiliary planes are shown as thick blue lines, while the *Top plane* is represented by a dashed line. For the creation of dentin, six out of eight planes (Planes 1-6) were used. A sketch of the tooth's cross-section is made on each of these planes. Using the *Loft* tool in SolidWorks, a solid body representing the dentin was constructed from the cross-section sketches. This step is illustrated in Fig. 2b. The *Loft* tool uses guide curves for solid body construction, seen in Fig. 2b as thick black curves with green marks at intersections with construction planes. The tooth's protrusions (cusps) are created using the *Free surface* feature on Plane 6. The CAD model of the dentin of the first lower premolar with its cusps is shown in Fig. 2c.

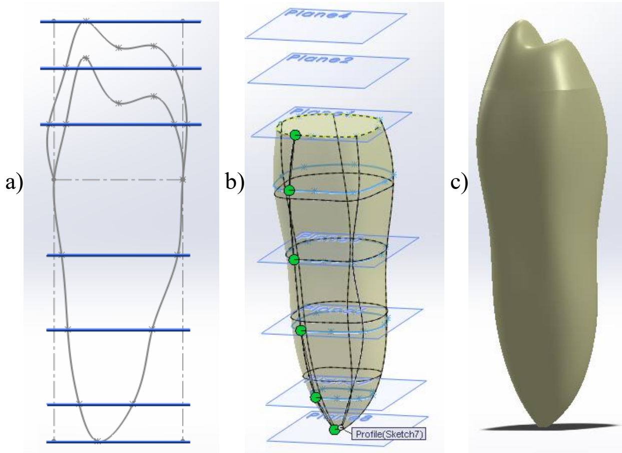

Figure 2. a) Sketch of dentin and enamel with parallel construction planes; b) cross-section sketches of dentin with guide curves from the Loft tool; c) dentin CAD model of the first lower premolar.

The enamel of the first lower premolar is constructed using the same principle. The first cross-section sketch of the enamel is made on the Top plane; the same one used for dentin. Figure 3a shows the formation of the solid body using the Loft tool. The cusps are made in the same manner as for the dentin. Using the indent feature, the dentin is embedded into the enamel, and the contact between dentin and enamel is established through the upper premolar surface of the dentin cusps. Figure 3b shows the final model of the lower first premolar replica and its cross-section.

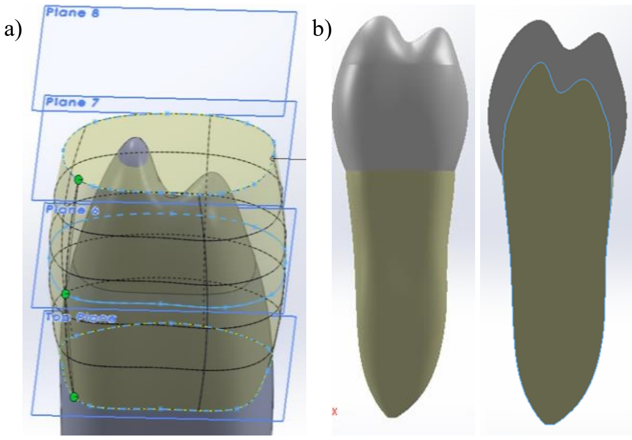

Figure 3. a) Construction planes and complementary cross-sections of the enamel; b) final model of first lower premolar and its cross-section.

Implant modelling

As part of this study, implant models are designed based on the Titamax GT implants. Primary differences between real Titamax GT implants and the CAD models used in this research are the threads, which were removed from the CAD models for the simplicity of analysis, and the abutments, which were omitted in both implant designs. The solid body of the implant consists of a cylinder with a diameter of 3.75 mm and length of 11 mm. The head of the implant is designed in the shape of a dome, utilising six auxiliary planes for its construction. The final implant CAD model and its cross-section are shown in Fig. 4.

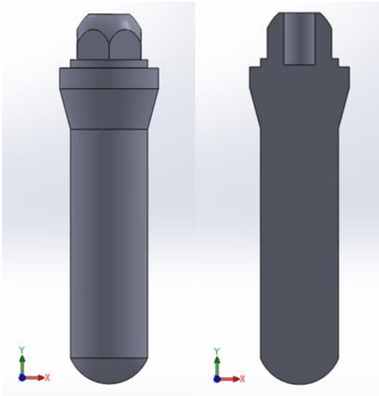

Figure 4. Implant CAD model without threads (left), and its cross-section (right).

First molar crown modelling

The first molar crowns were modelled directly on the implant. Specifically, in SolidWorks software, the implant model is imported initially, and then the crown is modelled onto it in the same manner as the previously performed dentin and enamel of the tooth. Using the indent feature, three separate solid bodies are defined that intersect with each other: the framework, the veneer, and the implant. The cusps of the crowns are also constructed using the freeform feature in SolidWorks. The crown of the first molar, together with the implant, is shown in Fig. 5. In this superstructure, the presence of an abutment, or support, is also disregarded.

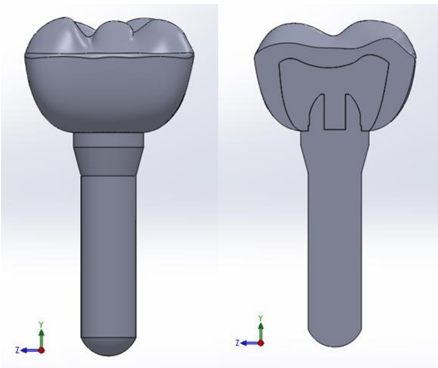

Figure 5. Implant with first molar crown (left), and its cross-section (right).

To complete the assembly, a 15×25×68 mm rectangular block is created, along with two rectangular supports measuring 5.08×25.4×38.1 mm each. The supports are positioned at two equidistant points to stabilise the block, creating a three-point bending configuration under the applied load. Similar supports are used in studies, /4-6/.

All created parts are imported into one assembly and placed within the rectangular block, positioned on the supports. The teeth and implants are placed as close to each other as possible without touching. In this study, the influence of interproximal contact is not taken into account; hence, the distance between adjacent crowns is not measured. Using the indent feature, the implants and tooth roots are embedded into the block, thereby fixing their positions. The final assembly with separated crowns is shown in Fig. 6a, and its cross-section in Fig. 6b.

a)

b)

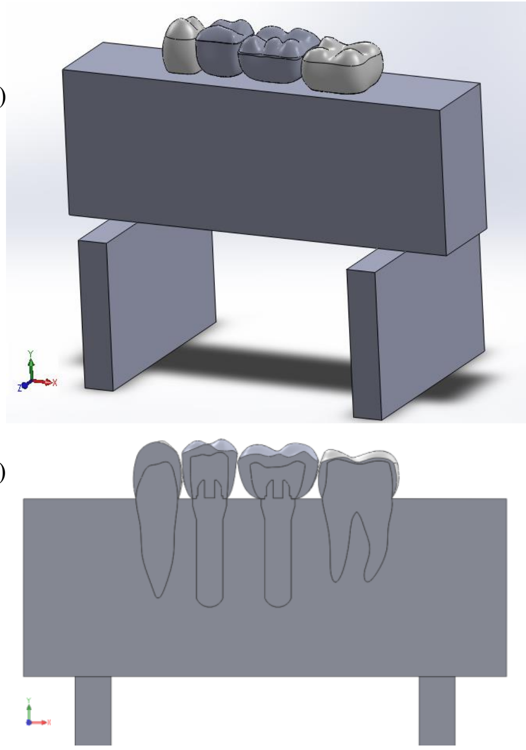

Figure 6. a) Final assembly with separated crowns; b) cross-section.

Since the only difference between the two constructed assemblies lies in the crowns, all other elements (i.e., first premolar, second molar, implants, rectangular block and supports) made for the assembly with separated crowns are used in the following assembly incorporating coupled crowns. Specifically, within this assembly, only the coupled crowns with veneers are created and placed on implants.

Coupled crowns assembly

To create the coupled crowns assembly, the implant model was first imported and then duplicated using the linear pattern feature at a distance of 10 mm, corresponding to the spacing between cylinder axes of implants. Further assembly involving crowns is carried out in the same manner as for the assembly with separated crowns.

The framework of the superstructure consists of three solids (obtained using a 3D sketch and Loft features), shown in Fig. 7, with cusps created using the freeform feature across the full surface of the framework can be observed.

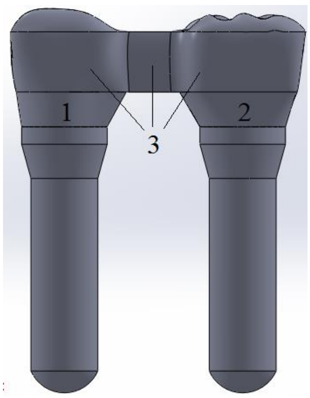

Figure 7. The framework of coupled crowns with marked solids obtained through the *Loft* feature.

The veneers of the coupled crowns are modelled in the same manner, utilising the same features in SolidWorks. Two implants with coupled crowns and their cross-section are shown in Fig. 8.

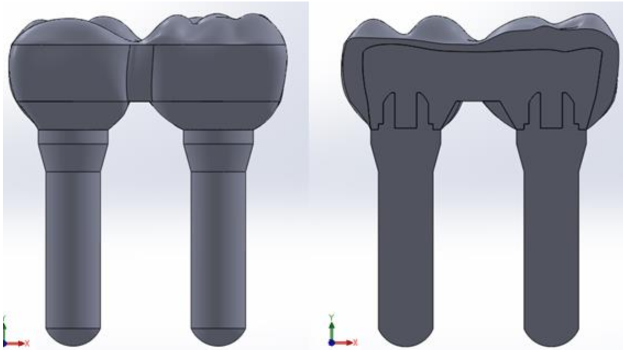

Figure 8. Coupled crowns of the second premolar and the first molar (left), and their cross-section (right).

The final assembly is formed in the same way as the assembly with separated crowns. All CAD models are imported and embedded into the rectangular block, thus creating an assembly. Final assembly with coupled crowns is shown in Fig. 9a, along with the corresponding cross-section view in Fig. 9b.

Within the scope of this study, the influence of the crown design, loading points, and veneer material on the mandible stress state is investigated using 8 computational models:

1. CCrv1x250 - coupled crowns, resin veneer, 1x250 N
2. CCpv1x250 - coupled crowns, porcelain veneer, 1x250 N
3. CCrv2x125 - coupled crowns, resin veneer, 2x125 N
4. CCpv2x125 - coupled crowns, porcelain veneer, 2x125 N
5. SCrv1x250 - separated crowns, resin veneer, 1x250 N
6. SCpv1x250 - separated crowns, porcelain veneer, 1x250 N
7. SCrv2x125 - separated crowns, resin veneer, 2x125 N
8. SCpv2x125 - separated crowns, porcelain veneer, 2x125 N

These assemblies are already used to examine the impact of veneer material choice /5/ and the effects of crown design /6/. The number of loading application points was also varied, ensuring that the total load never exceeds 250 N, as described in this paper. The load direction is vertical in all situations. In assemblies where the 250 N load is applied at one point, the application point is located on the crown of the first molar, in the area closer to the second molar, Fig. 10a and 11a. As for the assemblies with the 125 N load applied at two points, one application point is located on the crown of the first molar (identical to the 250 N case), while the second application point is on the crown of the second premolar, Fig. 10b and 11b. Both loading scenarios for the coupled crowns assembly and the separated crowns assembly are shown in Figs. 10 and 11, respectively. Figures also show boundary conditions, marked with orange and purple markers on supports, which will be explained in the following section.

a)

b)

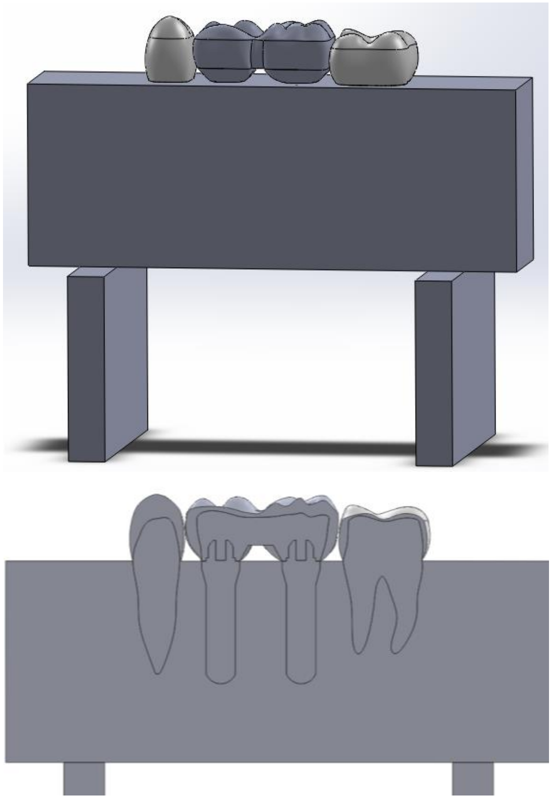

Figure 9. a) Final assembly with coupled superstructures; b) cross-section.

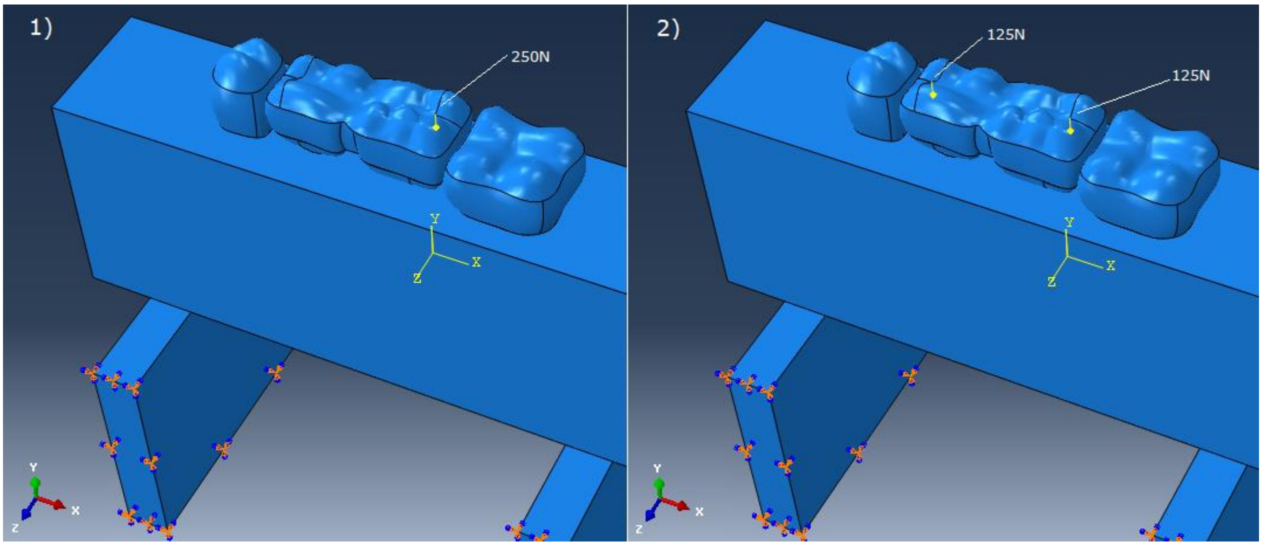

Figure 10. The assembly with coupled crowns: 1) single-point loading with 250 N in magnitude; 2) double-point loading with 125 N.

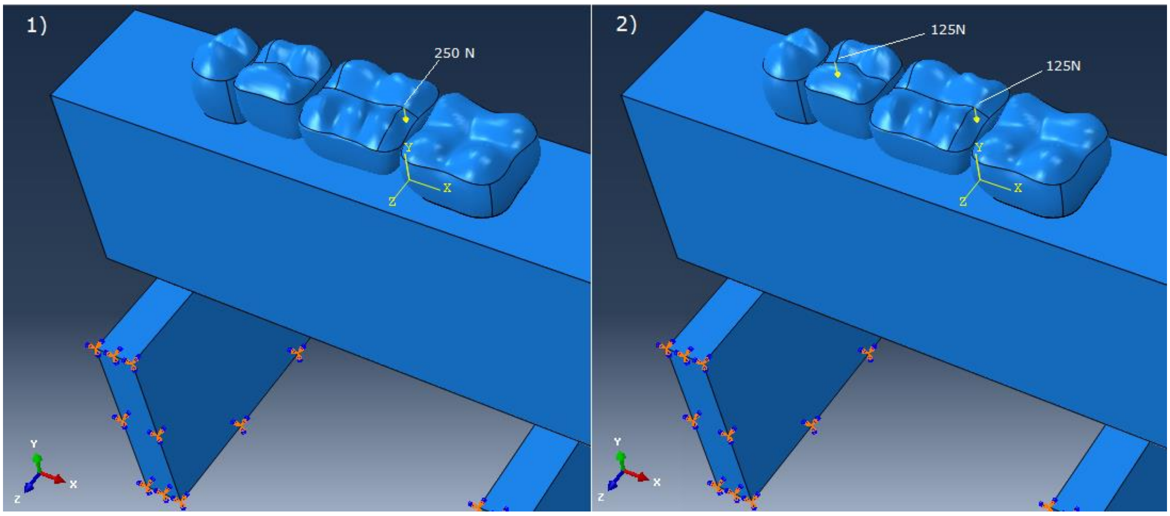

Figure 11. Assembly with separated crowns: 1) single-point loading with 250 N in magnitude; 2) double-point loading with 125 N.

Finite Element Analysis (FEA) of computational models

The FEA is performed using Abaqus® (Dassault Systèmes, Vélizy-Villacoublay, France) 6.10. Computational model analyses took between 5 and 15 min., depending on the model complexity. Boundary conditions for all computational models are set identically. Supports for the rectangular block are completely fixed, and the movement along the bottom surface of the rectangular block is restricted by the supports. All materials are considered linear elastic, with defined Young modules and Poisson ratio, /5/.

Computational model with coupled crowns consists of 245317 tetrahedral elements, whereas the model with separated crowns includes a total of 370669 tetrahedral elements. Difference in the total number of elements is due to different components used in the analysis. To ensure the most accurate results, the number of elements for the same component must remain approximately equal across different computational models. Hence, the implants at the position of the second premolar and the first molar have 9395 and 9557 elements in the computational model with separated crowns, respectively, while these two implants in the computational model with coupled crowns have 9456 and 9565 elements, respectively.

In the computational model with coupled crowns, the framework of the second premolar and the first molar is combined into a single unit consisting of 34687 elements, whereas in the computational model with separated crowns, the framework of the second premolar has 23019 elements, and the framework of the first molar has 90439 elements. The same applies to the veneers. The second premolar and first molar veneers in the computational model with coupled crowns have 32493 elements, while in the model with separated crowns, the second premolar veneer had 40924 elements, and the first molar veneer had 67214 elements.

RESULTS AND DISCUSSION

The results for the model CCpv1x250 are shown in Fig. 12, while the equivalent model subjected to two equal forces (i.e., 2×125 N) is presented in Fig. 13, both of which display the von Mises stress distribution. As expected, overall stress states are higher in the model with a single 250 N force, except for the maximal stress value which appears unexpectedly low. This discrepancy is likely due to post-processing limitations in ANSYS®, as extreme stress values are sometimes inaccurately visualised. In the 1×250 N force case, the maximal von Mises stress ranges from 80 to 531 MPa, while the counterpart in the 2×125 N case ranges from 100 to 503 MPa, with the higher value more likely in the latter. However, the more important observation is that the difference in stress distribution between single- and double-point loading scenarios is relatively minor, resulting from stress transfer through the coupled implants.

When focusing on stress in the implant body, difference becomes more pronounced. The maximal stress in the 1×250 N case reaches 94.7 MPa, approximately four times greater than the 23.6 MPa value recorded in the 2×125 N case. This can be explained by the following: in the single-force model, the entire load is transferred along the closer implant body, whereas in the dual-force model, the load is more evenly distributed between the two implant bodies.

The results for the SCpv1x250 model are shown in Fig. 14, while the equivalent model subjected to two forces (i.e., 2×125 N) is presented in Fig. 15. As expected, the model with a single 250 N force exhibits higher overall stresses, including the maximal value of 952 MPa, compared to the 752 MPa for the 2×125 N model. Similarly, the maximum stress in the implant body is notably higher in the single-force case (i.e., 173 MPa vs. 83 MPa), clearly indicating that separated implants have significantly higher stresses due to the absence of stress transfer between them.

One remaining point of uncertainty is the comparison between 503 MPa and 531 MPa, which is likely attributed to an unresearched bending effect in the models.

CONCLUSIONS

Based on the results presented in this study, it can be concluded that coupling the crowns and applying forces at two distinct points can significantly reduce stress concentrations within the implants and the surrounding mandibular structure. This highlights the biomechanical advantage of distributing occlusal loads across multiple points, especially in configurations with coupled implants.

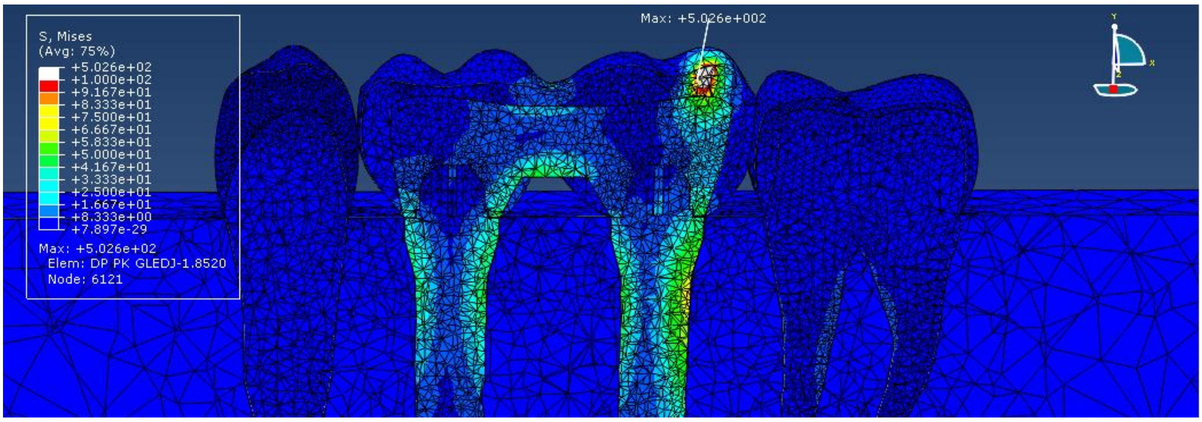

Figure 12. CCpv1x250 computational model, von Mises stress distribution.

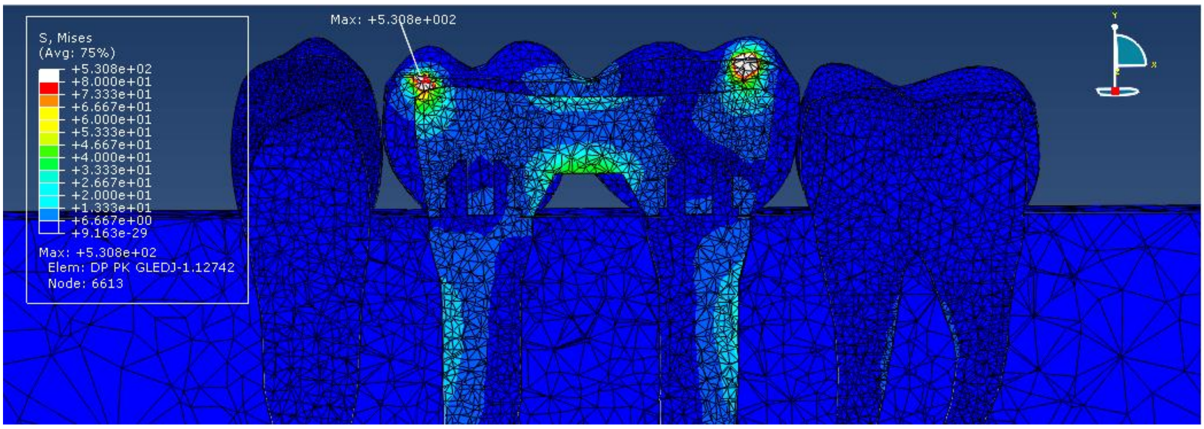

Figure 13. CCpv2x125 computational model, von Mises stress distribution.

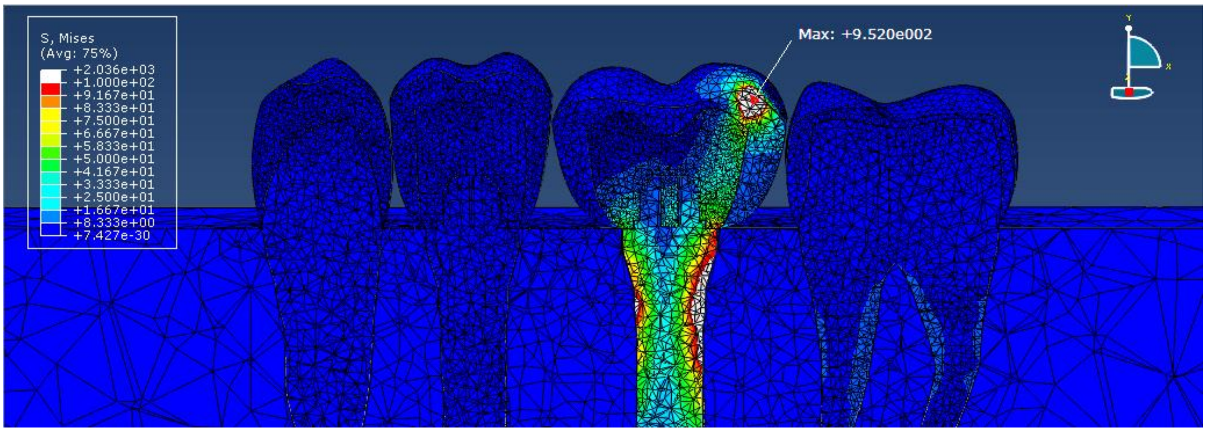

Figure 14. SCpv1x250 computational model, von Mises stress distribution.

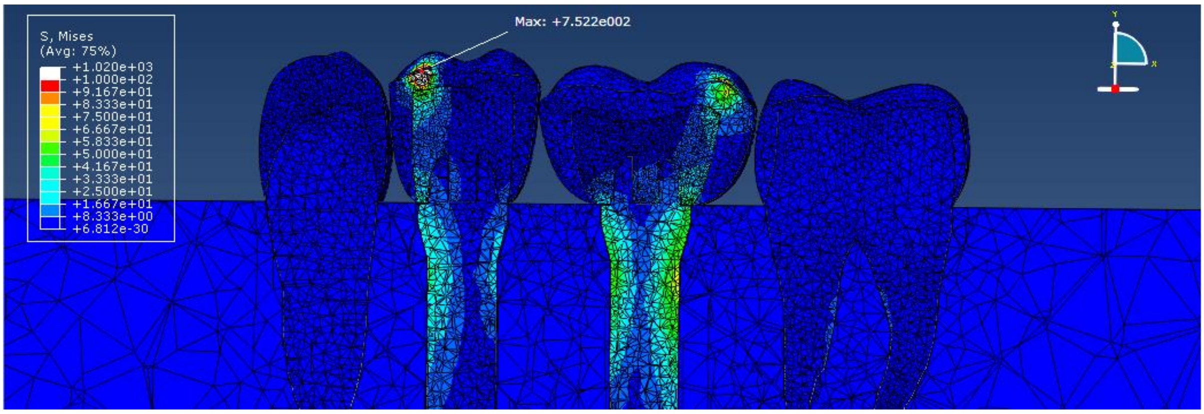

Figure 15. SCpv2x125 computational model, von Mises stress distribution.

Furthermore, the application of FEM has proven to be a valuable and reliable tool for numerically simulating stress distribution in the mandible, including its natural teeth and artificial structures such as dental implants. While *in vivo* testing remains highly challenging, FEM offers a non-invasive and flexible approach for evaluating the mechanical behaviour of various implant configurations. In particular, it enables comparative analysis between different artificial designs, loading scenarios, and material choices, providing meaningful insights that support clinical decision-making and guide the development of optimal restorative solutions.

ACKNOWLEDGEMENTS

The authors would like to thank the support from the Ministry of Science, Technological Development, and Innovation of the Republic of Serbia, under contract No. 451-03-136/2025-03/200213 (from February 4, 2025).

REFERENCES

1. Guichet, D.L., Yoshinobu, D., Caputo, A.A. (2002), *Effect of splinting and interproximal contact tightness on load transfer by implant restorations*, J Prosthet. Dent. 87(5): 528-535. doi: 10.1067/mpr.2002.124589
2. Tiossi, R., Lin, L., Rodrigues, R.C.S., et al. (2011), *Digital image correlation analysis of the load transfer by implant-supported restorations*, J Biomech. 44(6): 1008-1013. doi: 10.1016/j.jbiomech.2011.02.015
3. Tiossi, R., Lin, L., Conrad, H.J., et al. (2012), *Digital image correlation analysis on the influence of crown material in implant-supported prostheses on bone strain distribution*, J Prosthodont. Res. 56(1): 25-31. doi: 10.1016/j.jpor.2011.05.003
4. Tiossi, R., Vasco, M.A.A., Lin, L., et al. (2013), *Validation of finite element models for strain analysis of implant-supported prostheses using digital image correlation*, Dent. Mater. 29(7): 788-796. doi: 10.1016/j.dental.2013.04.010
5. Petrović, I., Sedmak, S., Tatić, U., et al. (2014), *Influence of choice of crown design on load transfer from implant to the bone*, J Manuf. Industr. Eng. 13(3-4): 1-3. doi: 10.12776/mie.v13i3-4.414
6. Sedmak, A., Milošević, M., Čolić, K., Petrović, I. (2023), *Effect of facet material on stress distribution in dental implants*, Struct. Integr. Life, 23(3): 363-366.
7. Geng, J.P., Tan, K.B., Liu, G.R. (2001), *Application of finite element analysis in implant dentistry: a review of the literature*, J Prosthet. Dent. 85(6): 585-598. doi: 10.1067/mpr.2001.115251
8. Clelland, N.I., Seidt, J.D., Daroz, L.G.D., McGlumphy, E.A. (2010), *Comparison of strains for splinted and nonsplinted implant prostheses using three-dimensional image correlation*, Int. J Oral Maxillofac. Implants, 25(5): 953-959.
9. Meijer, H.J.A., Kuiper, J.H., Starmans, F.J.M., Bosman, F. (1992), *Stress distribution around dental implants: influence of superstructure, length of implants, and height of mandible*, J Prosthet. Dent. 68(1): 96-102. doi: 10.1016/0022-3913(92)90293-j
10. Mitrović, N., Tanasić, I, Šarac, D., et al. (2016), *Analysis of the effect of implant distance from the surrounding structure in the PMMA block model*, Procedia Struct. Integrity 2: 1260-1265. doi: 10.1016/j.prostr.2016.06.161
11. Čolić, K., Sedmak, A., Vučetić, N., et al. (2024), *Finite element stress state analysis of mini dental implants*, Struct. Integr. Life, 24(1), 29-32. doi: 10.69644/ivk-2024-01-0029
12. Cicciù, M., Cervino, G., Bramanti, E., et al. (2015), *FEM analysis of mandibular prosthetic overdenture supported by dental implants: Evaluation of different retention methods*, Comput. Math. Methods Med. Article ID 943839. doi: 10.1155/2015/943839
13. Omori, M., Sato, Y., Kitagawa, N. et al. (2015), *A biomechanical investigation of mandibular molar implants: reproducibility and validity of a finite element analysis model*, Int. J Implant Dent. 1: 10. doi: 10.1186/s40729-015-0011-5